Control and Operation of Wind Turbine Converters during Faults in an Offshore Wind Power Plant Grid with VSC-HVDC Connection

S. K. Chaudhary, *Student Member, IEEE*, R. Teodorescu, *Senior Member, IEEE*, P. Rodriguez, *Senior Member IEEE*, P. C. Kjaer

***Abstract*—Voltage source converter (VSC) based high voltage dc (HVDC) transmission is an attractive technique for large offshore wind power plants, especially when long cable transmission is required for connection to the onshore grid. New multi-MW wind turbines are likely to be equipped with full scale converters to meet the stringent grid code requirements. In such a scenario, the offshore grid is terminated to the power electronic converters on all the ends.**

This paper presents a control scheme for the synchronization and control of the grid side converters (GSC) of the wind turbine generators (WTG). Current limit control enables the GSC to sustain the fault currents during short circuits in the offshore wind collector system grid. However, power transmission is affected, and the fault has to be isolated. It can be resynchronized after the fault has been cleared and the breaker reclosed. Healthy WTG converters can remain connected. The scheme is demonstrated through PSCAD/EMTDC simulation.

***Index Terms*—Wind power plants, symmetrical and symmetrical faults, over-current relays, wind turbine generators, VSC-HVDC.**

I. Introduction

THERE has been a tremendous growth in wind power industry in the last decade. In 2008, it grew by 31.7%, and the total installed capacity in the world reached 158.5 GW, out of which 76.2GW is in Europe [1]. There is a huge potential for offshore wind power generation. By 2020, EWEA targets to develop 230GW of wind power, with 40GW coming from offshore wind power plants [2].

Wind power plants require a large area as the individual generating unit size is only a few MW, around 5-6 MW at the most. Open seas can provide large areas with a more uniform and steady wind profile. Further there is less impact upon public tolerance like visual appearance, noise disturbance tower shadow etc. Therefore there is a growing interest to develop large offshore wind power plants (WPP). Europe had 43 fully operation offshore wind farms with a total output of 2396 MW by July 2010. At present the Thanet Offshore Wind farm, UK, comprising of 100 units of 3MW V90 wind turbine generators, spread over an area of approximately 35 sq. km.

Eventually, offshore wind power plants have to be connected to the onshore grid. High voltage ac cables generate a large reactive power, of the order of 1000kVAr/km for 132kV XLPE cables [3]. Voltage source based HVDC transmission is a suitable technology as DC cable transmission is not limited by the capacitive charging current as in the case of ac transmission. Moreover VSC-HVDC transmission offers a fast and independent control of active and reactive power in both directions. Further, it occupies a low footprint area, which is beneficial for offshore application.[4],[5] Long distance (200km) cable transmission was a reason to connect BorWin-I, the 400MW wind power plant, using VSC-HVDC.

The wind turbines spread over a wide area are connected to the collector bus through medium-voltage cables, typically at 30-36kV at the collector bus they are connected to the step up transformer. Depending upon the size and layout of the farm, there may be more than one collector bus in the offshore grid. Further the HVDC converter may be optimally placed between all the collector buses. The exact layout of the offshore grid is beyond the scope of this paper. Though a wind power plant is designed with enhanced reliability to minimize the fault incidents, the possibility of faults in the offshore wind power grid cannot be ruled out completely.

Permanent magnet generators have numerous advantages like absence of slip rings, multi-pole design for low speed operation, self-exciting characteristic and brushless design. These require full scale frequency converters, but the improved performance and overall decrease in cost of the machine as well as the power electronic converters have made PMG with full converters an attractive option [5]. These machines can be controlled over a wide speed range and hence have a better overall efficiency.

Most of the published literature describes the voltage ride through capabilities of doubly fed induction generator and the WTG with full scale converters [6-8]. Ref. [9] describes the grounding, overvoltage protection and insulation coordination in wind power plants. Protective relaying scheme for wind power plants is introduced in [10].

This work was supported by the Vestas Power Program, sponsored by Vestas Wind Systems A/S, Denmark.

S. K. Chaudhary and R. Teodorescu are with the Department of Energy Technology, Aalborg University, Aalborg E., 9220, Denmark (emails: skc@et.aau.dk, ret@et.aau.dk)

P. Rodriguez is with the Department of Electrical Engineering, Technical University of Catalunya, Barcelona, Spain. (email: prodriguez@ee.upc.edu)

P.C. Kjaer is with Vestas Wind Systems A/S, Dusager 4, Aarhus-8200, Denmark (pck@vestas.com).

978-1-4577-1002-5/11/$26.00 ©2011 IEEE

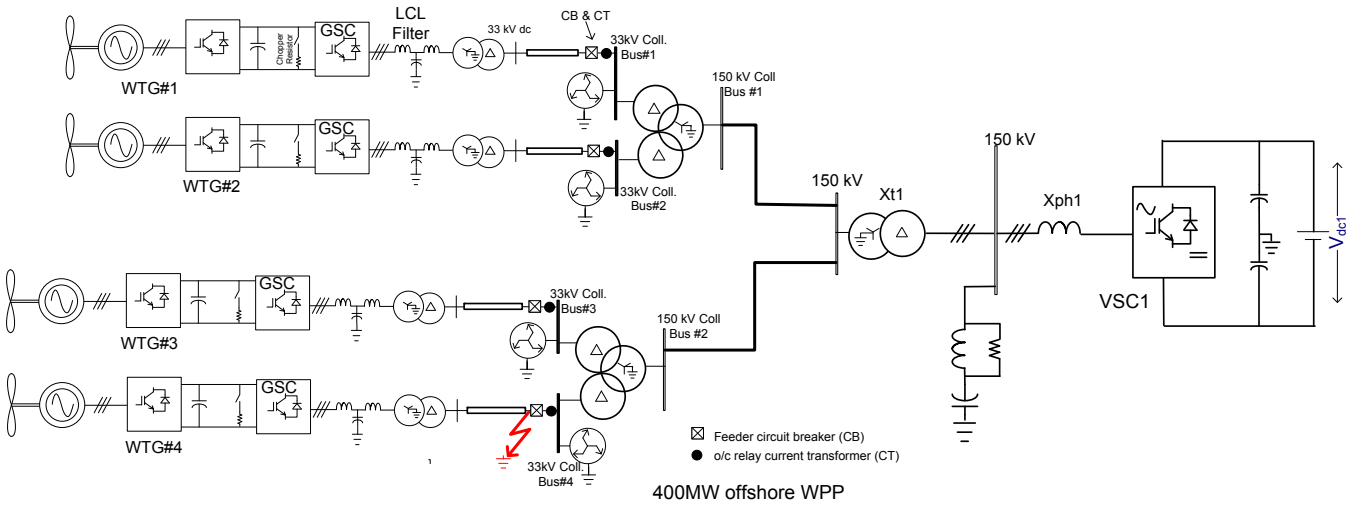

Fig. 1 Layout of an offshore wind power plant

There is lack of publication describing the control and operational aspects of wind turbine generator converter during the short circuit faults in the wind power plant collector grid. The short circuits may be asymmetrical one, involving a single phase or two phases or a symmetrical one involving all the three phases, and ground may or may not be involved.

In this paper, the control and operational aspects of the WTG with full scale converter is investigated in the event of short circuit faults in the offshore ac collector grid. The results are presented for a single line to ground (SLG) fault and triple line (LLL) fault. Fault is detected by the over-current relay in the feeder and isolated by the tripping of the circuit breaker. After the fault has been cleared, the circuit breaker is reclosed. WTG converter response during the fault and after the fault has been cleared has been described.

Section II describes a generalized offshore wind power grid layout. The WTG grid side converter controller is described in section III. Section IV gives the simulation results of the fault cases studied, followed by the conclusion in section V.

II. WPP Layout

A 400MW offshore wind power plant with VSC-HVDC connection to the onshore grid has been considered here as a study case. Fig. 1 provides the layout of the system. Only the offshore terminal of the VSC-HVDC has been shown here. Assuming that the assumption that the onshore VSC-HVDC terminal provides fast and efficient dc voltage regulation. Therefore, it is represented as a dc voltage source. A detailed switching model has been used for the offshore VSC-HVDC converter. It is a two level converter with sine-triangle modulation at 1950Hz switching frequency. The dc side voltage is 300kV, while the ac side voltage is 150kv rms. Phase reactor and the tuned filters have been modeled.

The offshore wind power grid comprise of two collector buses each with 3 winding transformers. Thus there are 4 collector buses (nos. 1, 2, 3and 4) at 33kV. Each 33kV collector bus is provided with a zig-zag connected grounding transformer [11]. The wind turbines are connected in cable feeders with a single breaker at the ends. For sake of simplicity, they have been represented as 4 aggregated wind turbines with their own LCL-filter, step up transformer, and 33kV cable section connecting to the collector bus through a breaker (Fig. 1).

The control schemes of the offshore VSC-HVDC terminal, and the grid side converter of the wind turbine generators have been described below.

A. Offshore VSC-HVDC controller

Offshore VSC-HVDC establishes the balanced three phase voltage profile at a constant frequency and magnitude. The controller is implemented in a rotating reference frame with the resultant voltage phasor aligned along the assumed d-axis. Therefore, d-axis voltage is controlled to 1 pu and the q-axis voltage is controlled to 0 pu reference. Inner current control loops are provided such that current limits can be enforced [12]. Fig 2 gives the block diagram of the offshore VSC-HVDC controller.

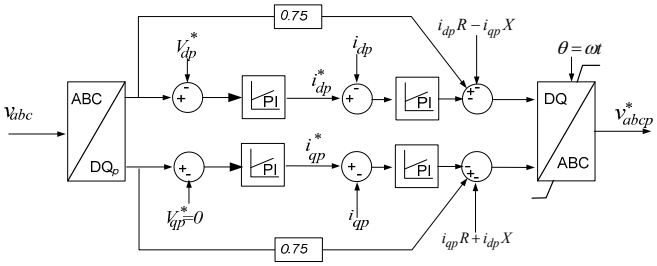

Fig. 2 Offshore VSC-HVDC Controller

B. Offshore WTG converter

The WTG is equipped with a back-to-back converter, which is referred as the full converter. The machine side converter controls the machine torque, thereby allowing a variable speed operation. The machine side converter (MSC) of the WTG along with the generator and the turbine is together represented by a constant power source with a first order time delay (of 10ms) has been assumed in the present simulation model. The power is supplied to the dc link and

hence, this power source has been represented by a current source in the simplified WTG model (Fig. 3). A chopper controlled braking resistor is provided to dissipate the excess power when the WTG-GSC is unable to evacuate the power due to fault or other problems in the collector ac grid.

The grid side converter (GSC) regulates the dc link voltage. As shown in Fig 4, the dc link voltage deviation is processed by a proportional-integral regulator to provide the active power reference to the GSC. Thus the generated active power is fed into the offshore grid. Reactive power can be independently absorbed or generated as per the operational requirement of the offshore grid, provided the current limit of the converter is not exceeded. In the present study, the reactive power reference has been arbitrarily set to 0.

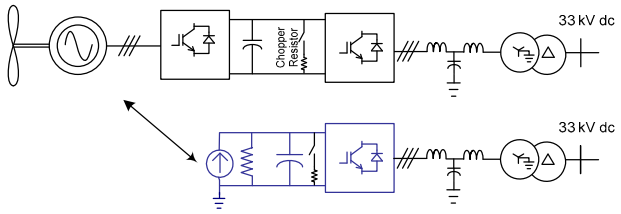

Fig. 3Model of an aggregated wind turbine generator with its LCL filter and step-up transformer.

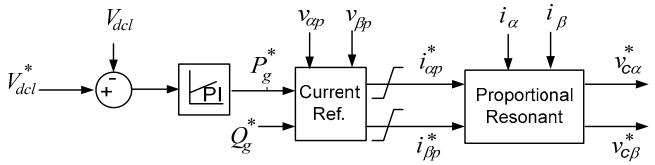

Fig. 4 WTG-GSC Controller in stationary reference frame

Using these references for the active and reactive power and the positive sequence components ($v_{\alpha p}$ and $v_{\beta p}$) of the WTG terminal voltage, the positive sequence output current references are generated and then proportional resonant controller is used to control the WTG-GSC (Fig. 4). It is described in detail in Section III.

III. Control of WTG-GSC

The WTG-GSC injects the active and reactive power into the offshore WPP grid. Therefore, it has to be synchronized with the offshore grid. Phase locked loop can be used to estimate the phase angle and frequency at the WTG terminal and then control the WTG-GSC. However, during faults and switching events, phase jumps are observed and the system undergoes through power transients. A controller in stationary reference frame can get rid of this problem, as phase estimation is not required, and frequency of the offshore grid is controlled at nominal value (say 50 Hz.) by the VSC-HVDC controller.

A. Estimation of Positive Sequence voltage at the WTG terminal

The measured 3 phase voltage at the capacitor bus in the LCL filter of the WTG is decomposed along the α–β axes in the stationary reference frame using Clarke's transformation (1).

$$\left.\begin{aligned} v_\alpha(t) &= \tfrac{2}{3}\left(v_a - 0.5v_b(t) - 0.5v_c(t)\right) \\ v_\beta(t) &= \tfrac{2}{3}\left(\tfrac{\sqrt{3}}{2}v_b(t) - \tfrac{\sqrt{3}}{2}v_c(t)\right) \end{aligned}\right\} \quad (1)$$

Second order generalized integrator (SOGI) is able to extract the in-phase components at the specified frequency and generate a component of the same rotated by a quadrature. Fig. 5 gives a block diagram of a SOGI quadrature signal generator (SOGI-QSG).

By Mason's loop gain formula, the transfer functions of the SOGI-QSG, tuned around the resonant frequency, ω are,

$$\left.\begin{aligned} \frac{V_\alpha(s)}{V'_\alpha(s)} &= \frac{k\omega s}{s^2+k\omega s+\omega^2} \\ \frac{qV_\alpha(s)}{V'_\alpha(s)} &= \frac{k\omega^2}{s^2+k\omega s+\omega^2} \end{aligned}\right\} \quad (2)$$

The parameter 'k' determines the bandwidth of the SOGI-QSG.

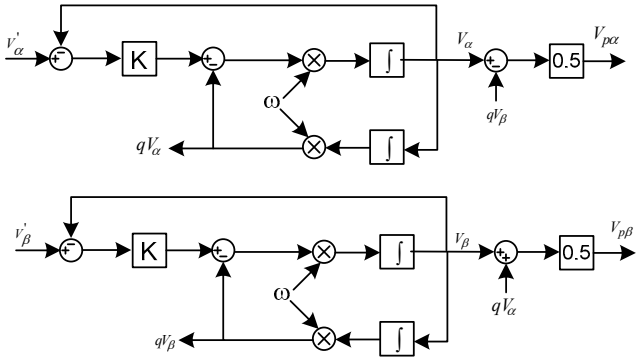

Fig. 5 Generation of positive sequence components using second order generalized integrator based quadrature signal generator (SOGI-QSG)

At, the tuned frequency, ω, the gains are unity.

$$\left.\begin{aligned} \left.\frac{V_\alpha(s)}{V'_\alpha(s)}\right|_{s=\pm j\omega} &= 1 \\ \left.\frac{qV_\alpha(s)}{V'_\alpha(s)}\right|_{s=\pm j\omega} &= -j \end{aligned}\right\} \quad (3)$$

The positive sequence components, $V_{p\alpha}$ and $V_{p\beta}$ along the $\alpha-\beta$ axes are given by the transformations (4) [13].

$$\begin{bmatrix} V_{p\alpha} \\ V_{p\beta} \end{bmatrix} = \tfrac{1}{2}\begin{bmatrix} 1 & -j \\ j & 1 \end{bmatrix}\begin{bmatrix} V_\alpha \\ V_\beta \end{bmatrix} \quad (4)$$

The most important advantage of this method is its non-dependence upon the measurement/estimation of phase angle. Moreover, the resonant frequency can be set around the nominal value of frequency set by the VSC-HVDC controller.

B. Determination of the positive sequence current references

DC-link voltage regulator of the WTG-GSC determines the reference active power to be evacuated (Fig. 6). The reactive power reference can be specified externally or it may be generated by some reactive power control logic. In the present case, reactive power reference has been arbitrarily set to 0.

The positive sequence current references for the WTG-GSC are given by the power relationship in the stationary reference frame (5).

$$\begin{bmatrix} i_{p\alpha}^* \\ i_{p\beta}^* \end{bmatrix} = \begin{bmatrix} v_{p\alpha} & v_{p\beta} \\ v_{p\beta} & -v_{p\alpha} \end{bmatrix}^{-1} \cdot \begin{bmatrix} P_g^* \\ Q_g^* \end{bmatrix} \quad (5)$$

A current limit is applied on the calculated current references, such that the resultant magnitude of the current remains within the safe limits of the converter.

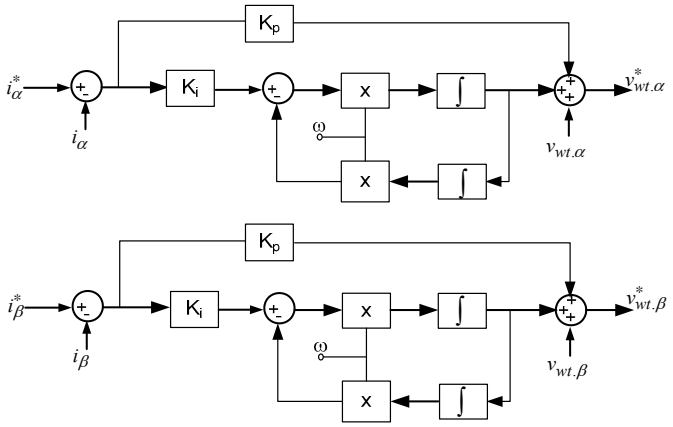

Fig. 6 Proportional resonant controllers for the WTG-GSC current control

C. Proportional resonant controllers for the WTG-GSC

Proportional resonant controllers are then used for the current control of the WTG-GSC (Fig. 6). The transfer function of the proportional resonant controller [14, 15] is given below (6). Eq. 7 shows the addition of LCL-filter capacitor voltages as feed-forward terms.

$$\left.\begin{aligned} v_{c\alpha}^* &= \left(K_p + \frac{K_i}{s^2+\omega^2}\right) \cdot \left(i_{p\alpha}^* - i_{p\alpha}\right) \\ v_{c\beta}^* &= \left(K_p + \frac{K_i}{s^2+\omega^2}\right) \cdot \left(i_{p\beta}^* - i_{p\beta}\right) \end{aligned}\right\} \quad (6)$$

$$\left.\begin{aligned} v_{wt.\alpha}^* &= v_{c\alpha}^* + v_{wtc.\alpha} \\ v_{wt.\beta}^* &= v_{c\beta}^* + v_{wtc.\beta} \end{aligned}\right\} \quad (7)$$

where,

α, β →subscripts for the $\alpha - \beta$ axes' components
v_c^* → Controller output references
v_{wtc} →LCL filter capacitor bus voltage of the WTG
v_{wt}^* →Output voltage reference for WTG-GSC.

D. Over-current Relay

An over-current relay with very inverse time characteristics can be used to detect and discriminate faults in the cable feeders connected to the collector bus. Since several WTG's are connected to a common cable feeder, they may be provided with a common circuit breaker, like in Horns Rev I [16]. When there is a short circuit fault in the feeder, the over-current relay should detect it and discriminate it against the healthy feeders. The relay should then trip the circuit breaker top isolate the fault. The following characteristics are particularly helpful in the process –

1. Each WTG-GSC is protected by its own current limit controllers.
2. VSC-HVDC is the largest in the wind power plant grid in terms of absolute ratings Therefore; it has the maximum contribution to the fault currents. Other WTG-GSC's also contribute to the fault current. Therefore high fault current contributions are observed from the collector bus side for a fault in the WTG cable feeder #4, as shown in Fig 1.
3. All the power electronic converters are capable of limiting their current output to their over-current limits, which is arbitrarily assumed here to be 1.10 pu for the WTG-GSC's and 15% for the VSC-HVDC converter. In the case of high impedance faults fault currents are low, and the relay pick up current can be tightly set.

Relay co-ordination studies are done to set the pick-up current ($I_{pick\text{-}up}$) and time dial setting such that proper discrimination is attained for the different types and strengths of faults. As per, IEEE Std. C37-112 [7], the over-current relay trip time, *t(I),* for the relay current transformer (CT) current '*I*' is given by,

$$\left.\begin{aligned} t(I) &= \left(\frac{A}{M^P - 1} + B\right) \\ where, M &= \left(\frac{I}{I_{pick_{up}}}\right) \end{aligned}\right\} \quad (8)$$

where, *A*, *B* and *P* are the constants defining the relay trip time characteristics, $I_{pick\text{-}up}$ is the relay pick up current setting. The trip time given by (8) is scaled by the time dial setting to obtain the actual trip time of the relay.

IV. SIMULATION OF FAULTS

VSC-HVDC system energizes the offshore wind power plant grid. The wind turbine generators get synchronized to this grid through their WTG-GSC. When the wind power plant is operating at its rated power generation, short circuit faults are simulated on the WTG cable feeder connected to the 33kV collector bus 4 (Fig. 1). Both symmetrical and asymmetrical faults have been simulated with two different fault resistance levels of (R_f) of 0.005pu and 0.25pu respectively. The fault duration is 150ms in all the cases..

The over-current relay has been tightly set with the pick-up current as 1.2pu and the time dial as 5ms. Eq. (8) gives the trip time of 225ms when the ratio, M is 1.2. The relay current transformers (CT) are placed at the 33kV collector bus end of the WTG feeders as shown in Fig 1. The faults are simulated on the feeder #4.

A delay of 50ms has been provided to simulate the opening time of the circuit breaker after the trip command has been received. The opening of the cable string circuit breaker also opens the WTG load break switches.

A. Single line to ground fault at a 33 kV collector bus, with R_f =0.005pu

Fig. 7 shows the current measured by the relay CT and the phase A at the time when the single line to ground (SLG) fault takes place. Grounding transformers enables the flow of fault current. The curves for power injected by different WTG-GSCs are shown in Fig. 8. The circuit breaker, which isolates the fault within 71 ms of the occurrence of the fault, is shown. It is reclosed at 4.35 s, after which the load switch of WTG gets closed with a delay of 50 ms. The GSC of WTG#4 then starts injecting power into the offshore grid. The plot shows that other WTG-GSCs get disturbed during the incidence of the fault, but as soon as the fault is cleared by the circuit breaker opening they resume operation.

Fig. 9 shows the phase 'A' voltage waveform during the fault and after it has been cleared. Voltage recovers immediately after the circuit breaker is opened. A small disturbance is observed when the circuit breaker is reclosed. An overvoltage of the order of 1.64 pu is observed. Fig. 10 shows that WTG#1 GSC gets affected for a very short time during the fault and normal operation resumes as soon as the circuit breaker isolates the fault. Since WTG#4 gets isolated by the circuit breaker, the positive sequence voltage decays below the threshold (0.25 kV that is 9.3% of the nominal voltage was arbitrarily set as the threshold for blocking the WTG-GSC). For the GSC of WTG#4, there is some delay in the rise of currents due to the dynamics of the SOGI-QSG positive sequence estimator.

B. Triple line fault at a 33 kV collector bus, with R_f=0.005pu

The fault current and the voltage waveforms during the appearance of a three phase symmetrical fault (LLL-fault) are shown in Fig. 11. Peak fault currents are found to be lower than those observed for the SLG fault and hence the relay trip time is longer. The circuit breaker opens in 87ms and the voltage recovers quickly. As a result of this the healthy WTG-GSC's resume normal operation. WTG#4 gets isolated due to the fault on the cable. Only after the fault has been cleared and the circuit breaker reclosed, it gets re-synchronized and starts injecting power into the offshore grid. The healthy WTG's observe power interruption for a short time prior to fault isolation by the opening of the circuit breaker (Fig. 12). The voltage and currents at the healthy WTG-GSC normalize soon after the opening of the breaker. WTG#4-GSC takes some time to resynchronize after its breakers have been closed and terminal voltage has reappeared as shown in Fig. 13. Since the dc link voltage regulator is saturated, its output power rises to very high values. This may be improved by limiting the rate of rise of output power, but that was beyond the scope of this study.

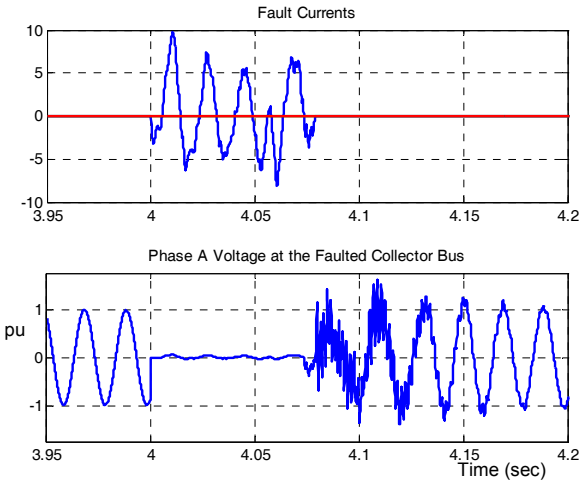

Fig. 7 Fault Current and voltage (in pu) at the 33kV faulted collector bus for SLG-fault with R_f =0.005 pu. [CB opens at 4.071s]

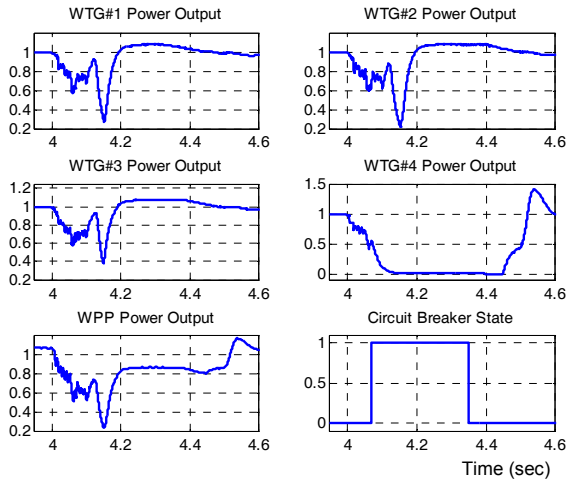

Fig. 8 Output power (in pu) of the WTG converters and the circuit breaker state for the SLG-fault with R_f =0.005 pu [CB opens at 4.071s, recloses at 4.348s]

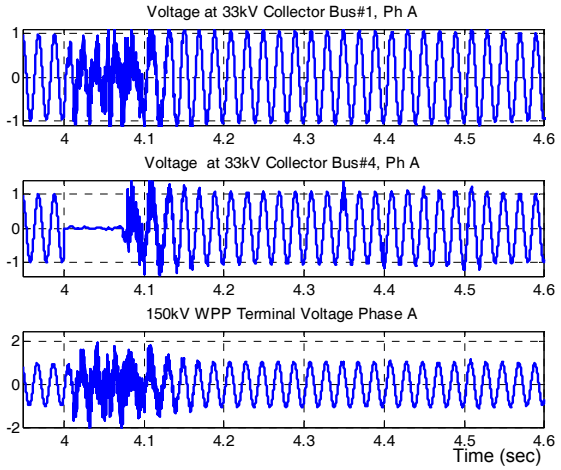

Fig. 9 Phase 'A' voltage waveforms (in pu)at the collector bus #1 and #4 for the SLG-fault with R_f =0.005 pu. [CB opens at 4.071s, recloses at 4.348s]

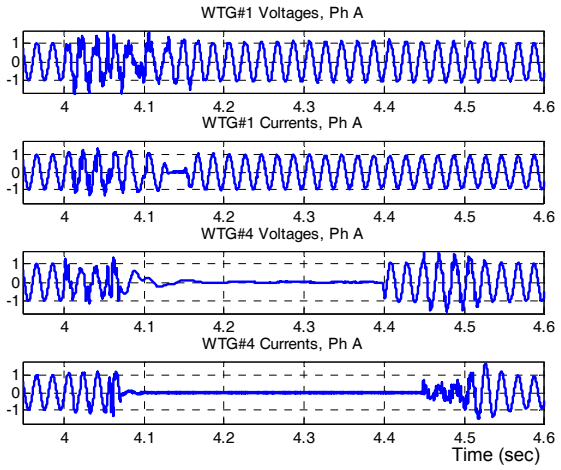

Fig. 10 Phase 'A' currents and voltages (in pu) of WTG#1 and WTG#4 for the SLG fault with R_f =0.005 pu. [CB opens at 4.071s, recloses at 4.348s]]

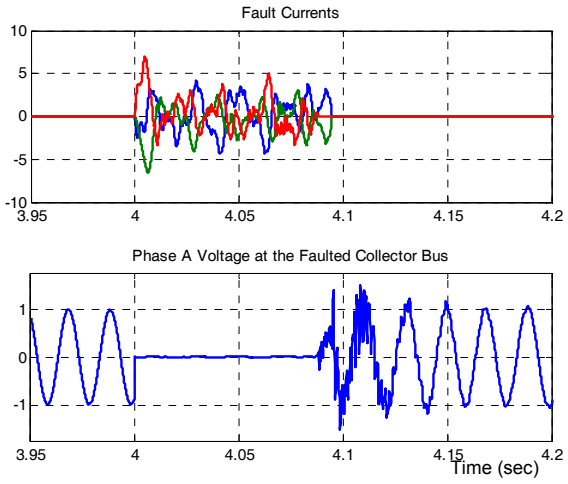

Fig. 11 Fault Current and voltage (in pu) at the 33kV faulted collector bus for LLL-fault with $R_f = 0.005$ pu. [CB opens at 4.087s]

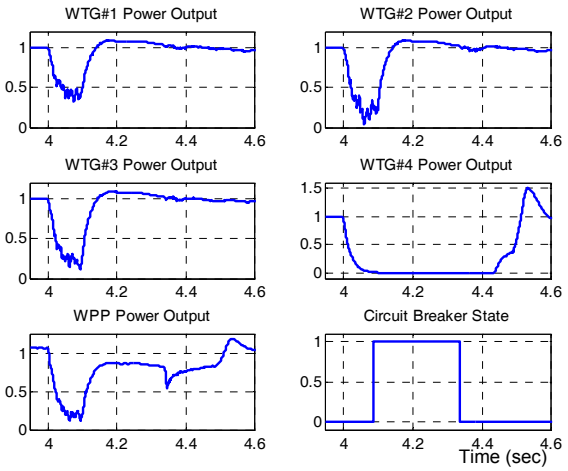

Fig. 12 Output power (in pu) of the WTG converters and the circuit breaker state for the LLL-fault with $R_f = 0.005$ pu [CB opens at 4.087s, recloses at 4.336 s]

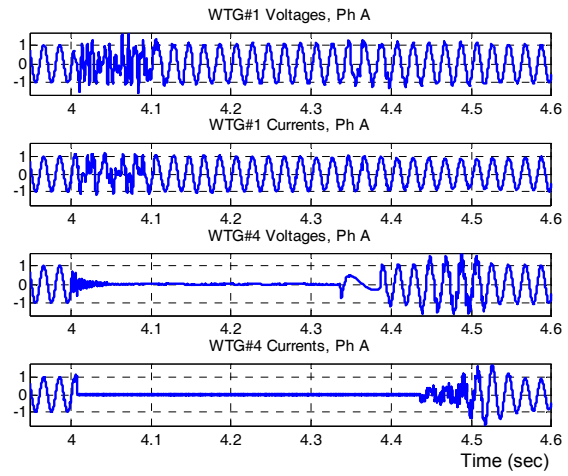

Fig. 13 Phase 'A' currents and voltages (in pu) of WTG#1 and WTG#4 for the LLL-fault with $R_f = 0.005$ pu. [CB opens at 4.087s, recloses at 4.336 s]

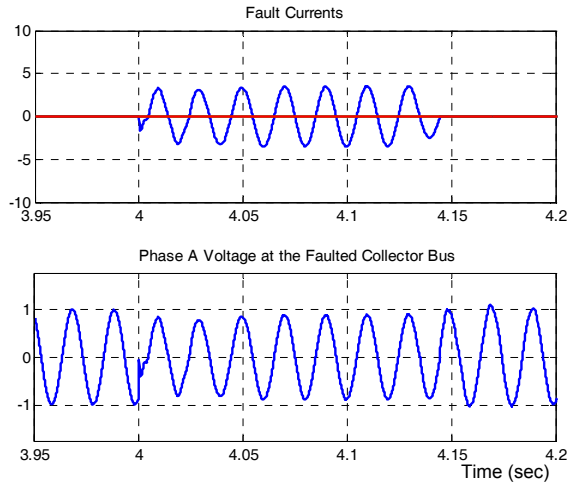

pu

Fig. 14 Fault Current and voltage (in pu) at the 33kV faulted collector bus for SLG-fault with $R_f = 0.25$ pu. [CB opens at 4.134s]

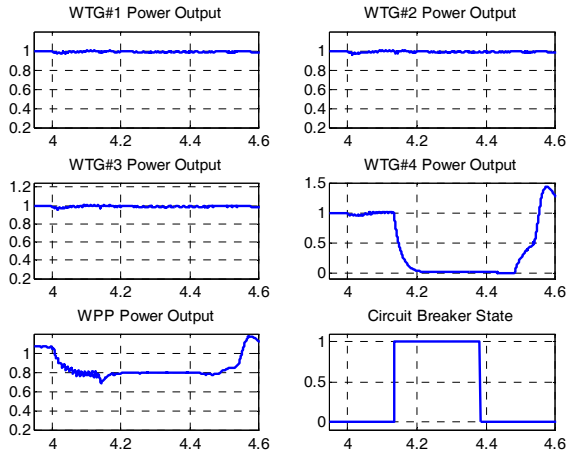

Fig. 15 Output power (in pu) of the WTG converters and the circuit breaker state for the SLG-fault with $R_f = 0.25$ pu [CB opens at 4.134s, recloses at 4.382 s]

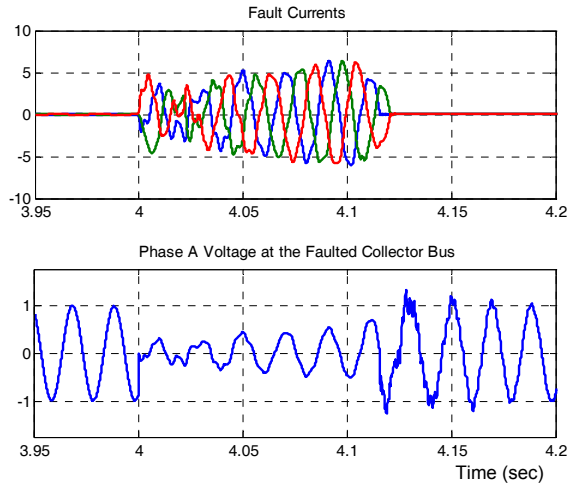

Fig. 16 Fault Current and voltage (in pu) at the 33kV faulted collector bus for LLL-fault with $R_f = 0.25$ pu. [CB opens at 4.106s]

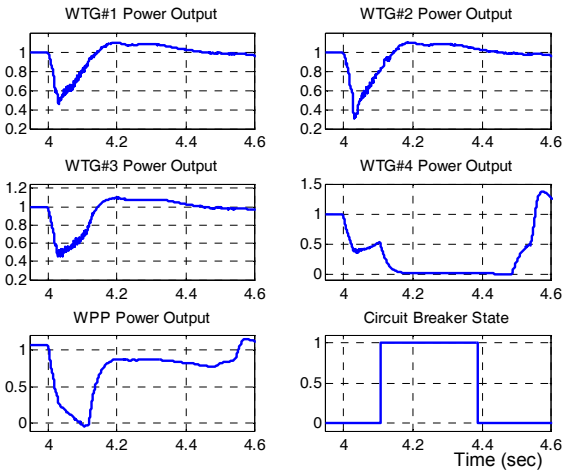

Fig. 17 Output power (in pu) of the WTG converters and the circuit breaker state for the LLL-fault with R_f =0.25 pu [CB opens at 4.106s, recloses at 4.386 s]

C. Single line to ground fault at a 33 kV collector bus, with R_f=0.25pu

Fault currents are lower when the fault resistance is high (0.25 pu in this case). Consequently, the over-current relay trip time is longer and the fault disconnected after 134ms, at the instant 4.134s (Fig. 14). However, the power generation by the wind turbine generators remain at around their nominal values, though the overall power generation by the wind power plant is found to fall by 20% in this case. This power gets lost into feeding the fault. After the fault is isolated by the opening of the circuit breaker, the remaining wind turbine generators contribute to the output of the wind power plant. The isolated WTG#4 has to be resynchronized before its normal operation resumes (Fig. 15).

D. Triple line fault at a 33 kV collector bus, with R_f =0.25pu

In this case the fault currents are higher, than those observed in the case of SLG faults (with same R_f=0.25 pu) and hence the relay operation is faster. The circuit breaker opens in 106ms, at the time instant 4.106s (Fig. 16). Power evacuation in all the WTG converters is affected. Overall power output of the WPP is badly affected as long as the fault persists, as the net power output of the falls to negative levels (Fig. 17). This implies that the VSC-HVDC is feeding the fault to some extent. The situation improves after the fault is isolated by the over-current relay tripping the circuit breaker.

V. DISCUSSION

VSC-HVDC provides the synchronizing voltage reference to the wind farm. Since the offshore ac collector grid frequency is controlled by the VSC-HVDC controller, the frequency is known beforehand. Therefore, the SOGI-QSG and proportional resonant controllers can be tuned to the offshore grid frequency and there is no need of any frequency estimation. When there is a fault in the offshore WPP collector grid, the HVDC connection would mean that the onshore ac grid remains isolated. Depending upon the severity of the fault, the offshore grid voltage gets affected as long as the fault remains connected.

VSC-HVDC is the largest converter in the offshore grid as it is designed to evacuate all the power generated by the whole wind power plant. Hence, this provides the maximum contribution to the short circuit faults in the offshore grid, even though its own controller limits the over-current level on its own base. The high fault current contribution from the VSC-HVDC helps in discriminating the fault location. At the same time, the maximum fault current provided by the VSC-HVDC is predictable as it is limited to its own over-current rating.

Another advantage of VSC-HVDC system, in the case of offshore wind power plants, is that as soon as the fault is cleared it restores the voltage profile in the offshore collector bus system. Thus, the healthy WTG feeders can resume their injection of the generated wind power to the VSC-HVDC transmission.

VI. CONCLUSION

The study shows the control and operation of the WTG-GSC in the event of fault in the cable feeders connecting several WTG in a string. The WTG-GSC is controlled to evacuate the excess power from the dc link of the WTG full converter. Only positive sequence current injection has been considered for the WTG-GSC. Proportional resonant controllers, tuned at nominal frequency (50 Hz), are used to drive the positive sequence current references in the stationary reference frame.

Control and operation of WTG-GSC during the faults has been demonstrated through simulation. There is power interruption in presence of severe faults. However, heavy fault currents can be detected fast by the over-current relay and the circuit breaker can be tripped sooner to isolate the fault. Soon after the fault is isolated, the remaining part of the circuit resumes injecting power into the offshore grid which can be evacuated by the VSC-HVDC transmission. The isolated WTG goes into blocking state as the positive sequence component of its terminal voltage falls below the threshold level. It can be resynchronized after the fault has been cleared, the circuit breaker reclosed, thereby resulting in the buildup of the positive sequence voltage at nominal frequency.

VII. REFERENCES

[1] Global Wind Energy Council, “Global Wind 2009 Report,”, March 2010. Available at: http://www.gwec.net

[2] European Wind Energy Association, “Pure Power Wind Energy Targets for 2020 and 2030,” 2009 update. Available at: http://www.ewea.org

[3] S. D. Wright, A. L. Rogers, J. F. Manwell, and A. Ellis, “Transmission options for offshore wind farms in the United States,” 2002. [Online]. Available at http://www.ecs.umass.edu

[4] Bresesti, P.; Kling, W.L.; Hendriks, R.L.; Vailati, R.; , "HVDC Connection of Offshore Wind Farms to the Transmission System," *IEEE Trans. Energy Conversion,* , vol.22, no.1, pp.37-43, March 2007

[5] H. Li, and Z. Chen,, "Overview of different wind generator systems and their comparisons," *Renewable Power Generation, IET* , vol.2, no.2, pp.123-138, June 2008

[6] C. Feltes, H. Wrede, F.W. Koch, and I. Erlich, “Enhanced Fault Ride-Through Method for Wind Farms Connected to the Grid Through VSC-Based HVDC Transmission,” *IEEE Trans. Power Systems*, vol. 24, Aug. 2009, pp. 1537-1546.

[7] G. Ramtharan, A. Arulampalam, J.B. Ekanayake, F.M. Hughes and N. Jenkins, "Fault ride through of fully rated converter wind turbines with

AC and DC transmission," *Renewable Power Generation, IET* , vol.3, no.4, pp.426-438, December 2009

[8] A.D. Hansen and G. Michalke, "Multi-pole permanent magnet synchronous generator wind turbines' grid support capability in uninterrupted operation during grid faults," *Renewable Power Generation, IET* , vol.3, no.3, pp.333-348, Sept. 2009

[9] IEEE PES Wind Plant Collector System Design Working Group, "Wind power plant grounding, overvoltage protection, and insulation coordination:"," *Power & Energy Society General Meeting, 2009. PES '09. IEEE* , vol., no., pp.1-8, 26-30 July 2009

[10] IEEE PES Wind Plant Collector System Design Working Group, "Wind plant collector system fault protection and coordination," *IEEE PES Transmission and Distribution Conference and Exposition 2010,* , vol., no., pp.1-5, 19-22 April 2010

[11] R. Van de Sandt, J. Lowen, J. Paetzold, and I. Erlich, "Neutral earthing in off-shore wind farm grids," *PowerTech, 2009 IEEE Bucharest* , vol., no., pp.1-8, June 28 2009-July 2 2009.

[12] L. Xu, B. W. Williams and L. Yao, "Multi-terminal DC transmission systems for connecting large offshore wind farms," *Power and Energy Society General Meeting - Conversion and Delivery of Electrical Energy in the 21st Century, 2008*.

[13] M. Ciobotaru, R. Teodorescu, and F. Blaabjerg, "A New Single-Phase PLL Structure Based on Second Order Generalized Integrator," *37th IEEE Power Electronics Specialists Conference, 2006. PESC '06.*, 18-22 June 2006

[14] F. Blaabjerg, R. Teodorescu, M. Liserre and A.V. Timbus, "Overview of Control and Grid Synchronization for Distributed Power Generation Systems," *IEEE Trans. Industrial Electronics,* vol.53, no.5, pp.1398-1409, Oct. 2006

[15] R. Teodorescu, F. Blaabjerg, M. Liserre, and P.C. Loh, "Proportional-resonant controllers and filters for grid-connected voltage-source converters," *IEE Proc. Electric Power Applications*, vol.153, no.5, pp.750-762, September 2006

[16] P. Christiansen, K. Jorgensen, and A.G. Sorensen, "Grid Connection and Remote Control for the Horns Rev 150 MW Offshore Wind Farm in Denmark," Available at http://www.hornsrev.dk

[17] *IEEE Standard Inverse-Time Characteristic Equations for Over-current Relays*, IEEE Std C37.112-1996, Sep. 1996.